

Recent developments in plasma spray processes for applications in energy technology

G Mauer, M O Jarligo, D Marcano, S Rezanka, D Zhou and R Vaßen

Forschungszentrum Jülich GmbH, Institute of Energy and Climate Research,
IEK-1: Materials Synthesis and Processing, 52425 Jülich, Germany

Abstract. This work focuses on recent developments of plasma spray processes with respect to specific demands in energy technology. High Velocity Atmospheric Plasma Spraying (HV-APS) is a novel variant of plasma spraying devoted to materials which are prone to oxidation or decomposition. It is shown how this process can be used for metallic bondcoats in thermal barrier coating systems. Furthermore, Suspension Plasma Spraying (SPS) is a new method to process submicron-sized feedstock powders which are not sufficiently flowable to feed them in dry state. SPS is presently promoted by the development of novel torch concepts with axial feedstock injection. An example for a columnar structured double layer thermal barrier coating is given. Finally, Plasma Spray-Physical Vapor Deposition (PS-PVD) is a novel technology operating in controlled atmosphere at low pressure and high plasma power. At such condition, vaporization even of high-melting oxide ceramics is possible enabling the formation of columnar structured, strain tolerant coatings with low thermal conductivity. Applying different conditions, the deposition is still dominated by liquid splats. Such process is termed Low Pressure Plasma Spraying-Thin Film (LPPS-TF). Two examples of applications are gas-tight and highly ionic and electronic conductive electrolyte and membrane layers which were deposited on porous metallic substrates.

1. Introduction

Material development covers material synthesis on the one hand and processing techniques on the other hand. These scopes are closely related to each other and must be both considered correspondingly [1]. With respect to energy technology, some present development goals are strain tolerant microstructures with low thermal conductivity, thin and gas tight functional layers, and processing of new materials with particular difficulties such as decomposition and inhomogeneous evaporation.

In this work, three recent developments of plasma spray processes are introduced with respect to some demands in energy technology. Processing of MCrAlY bondcoats for TBCs by High Velocity-Atmospheric Plasma Spraying (HV-APS) was established as an alternative to common processes such as Low Pressure Plasma Spraying (LPPS) or High Velocity Oxy-Fuel Spraying (HVOF). HV-APS manufactured microstructures, phase compositions and oxygen contents were investigated with respect to their impact on oxidation behaviour. Moreover, the processing of nano-sized powder feedstock by Suspension Plasma Spraying (SPS) is described as a processing method to obtain new microstructures such as dense vertically cracked or columnar structured ceramic thermal barrier coatings (TBCs). Finally, the processing of oxide ceramics by Plasma Spray-Physical Vapor Deposition (PS-PVD) is shown to obtain novel microstructures such as strain tolerant, columnar structured TBCs on the one hand as well as thin and dense gas separation membranes and electrolytes on the other hand.



2. High Velocity-Atmospheric Plasma Spraying

MCrAlY alloys are typically applied to protect e. g. gas turbine components from high temperature oxidation and to promote the bonding of ceramic thermal barrier coatings [2, 3]. The basic constituents are M=Ni, Co or a combination thereof, further alloying elements are 17–30% Cr, 8–15% Al and smaller amounts of reactive elements such as Y. MCrAlY coatings should exhibit a low porosity, a sufficient low oxygen content, and a controlled oxidation behaviour. Typical coating processes are LPPS (formerly often termed VPS), HVOF, and sometimes APS. HV-APS however, aims to offer an alternative method operated under atmospheric conditions but without oxygen as process gas. Furthermore, particle temperatures can be well adjusted as high as necessary but as low as possible. High particle velocities are obtained at justifiable costs as the gas consumption is much lower compared to other kinetic spray processes [4].

2.1 Process development

The HV-APS process was realized applying a TriplexPro™-210 torch (Oerlikon Metco AG, Wohlen, Switzerland) equipped with a 5 mm nozzle. The plasma gas flow was increased to the maximum possible values of 190 slpm Ar and 40 slpm He. Higher flows were not available due to limitations of the spray facility and gas supply. The current was increased to 450 A which is the highest value being allowed to be applied with the 5 mm nozzle according to the torch specifications. Figure 1 shows a plasma jet under HV-APS conditions. Since the flow is supersonic, the characteristic sequence of compression and expansion cells (shock diamonds) is generated.

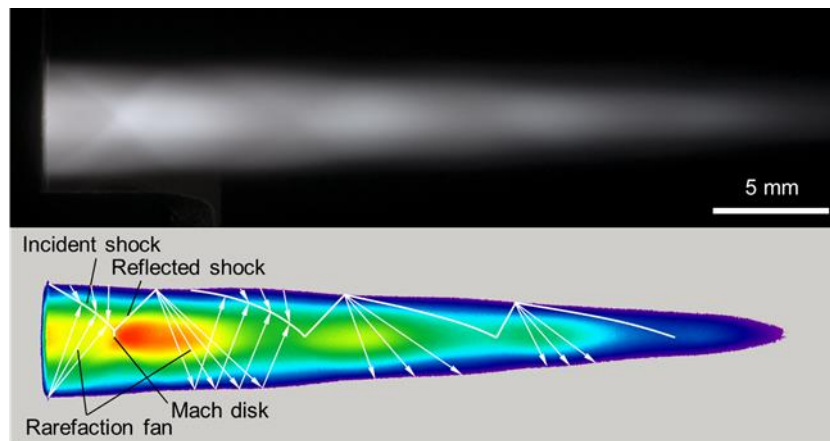


Figure 1. Shock diamonds in a supersonic HV-APS plasma jet.

Initially, the Co-32Ni-21Cr-8Al-0.5Y powder feedstock was optimized. As a result, a very fine cut (-22 / +5 μm) was selected. The carrier gas flow had to be increased up to 6.5 slpm in order to achieve an appropriate injection depth of the fine powder particles into the high-velocity plasma jet. The lowest coating porosities and best deposition efficiencies were observed at a spray distance of 100 mm.

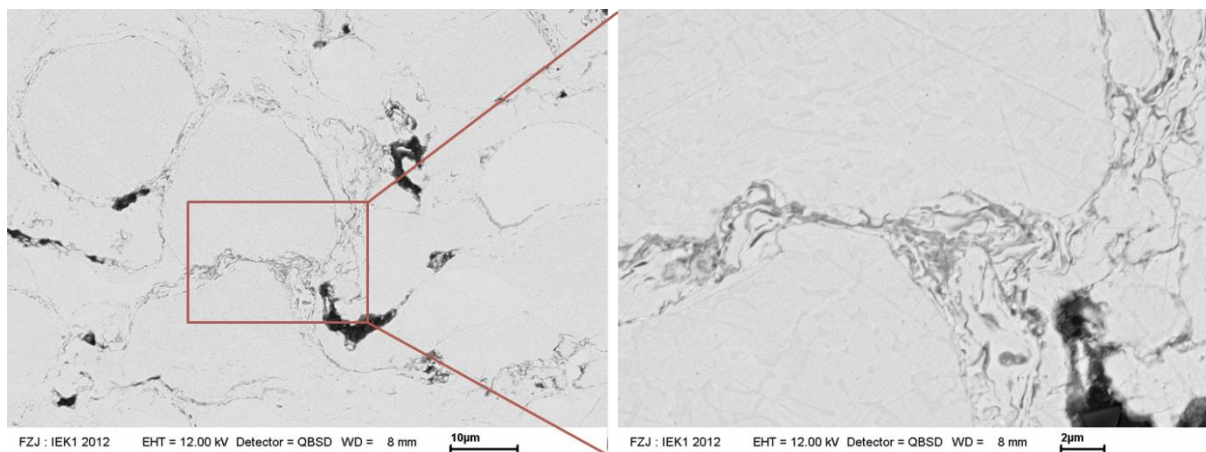


Figure 2. HV-APS as-sprayed microstructures [4].

Figure 2 gives insight into the microstructures obtained at these parameters. It is obvious that the powder particles were softened just so much that a dense structure could be achieved. On the other hand, particle temperature was low enough to avoid extensive oxidation; during the short flight time, only a thin oxide scale was formed on the particle surfaces. A chemical analysis revealed an oxygen content of 0.41 ± 0.04 wt% which is more than what is typically obtained by LPPS [5]. However, it is much less than obtained by APS [6] and lower compared to most of the HVOF coatings [7]. By HVOF, lower oxygen contents are still possible, but only using a much coarser powder feedstock [8]. However, allowances have to be made with respect to a small porosity.

2.2 Oxidation tests

Isothermal oxidation tests were performed with freestanding coating specimen at 1100°C in synthetic air for 72 h [9]. HV-APS samples were compared with LPPS reference samples. Despite their higher oxygen content, the HV-APS samples showed a distinctly lower oxidation rate, Figure 3. The aluminium-rich beta phase was less depleted and the thermally grown oxide layer (TGO) was thinner, more homogeneous, and consisted of virtually pure alumina.

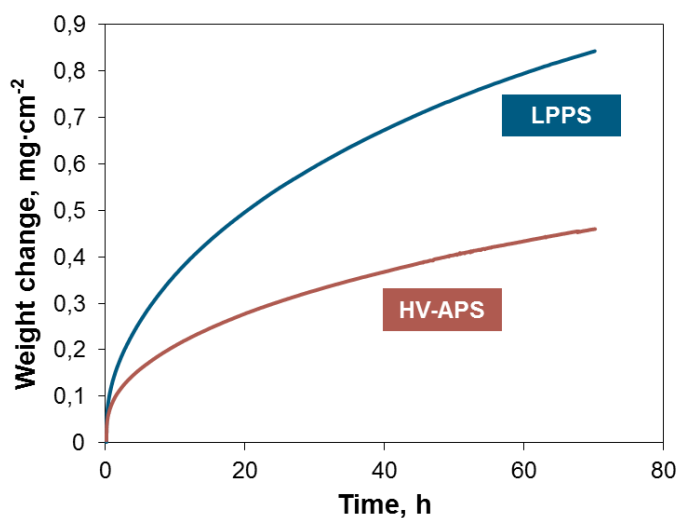


Figure 3. Isothermal oxidation rates of freestanding HV-APS and LPPS coating specimen at 1100°C in synthetic air for 72 h [9].

So called Y-Al oxide pegs, as they are typically formed in LPPS coatings, were missing in the HV-APS samples, Figure 4. Y was present in form of nano-sized oxide particles. No obvious depletion of Y-rich oxides occurred during oxidation. In contrast, in the LPPS reference samples, Y was present in Ni-Y intermetallic phases. It was used up during oxidation. This unique, new distribution of Y-rich nano-sized oxide precipitates in the HV-APS samples was able obviously to moderate the thermal growth of the oxide layer. Positive effects were also revealed for cyclic oxidation. Tests (2 h cycles) at 1100 °C in laboratory air for 300 h confirmed the better oxidation resistance of the HV-APS coatings. The LPPS specimen even showed indications of delaminated oxide scales at the edges. This was not the case for the HV-APS coatings which obviously did not reach a critical thickness of the TGO layer [10].

Hence, HV-APS appears to be a promising, cost effective alternative to established spraying techniques such as LPPS and HVOF. However, the formation mechanisms of the particular oxide distribution and the effect on the oxidation behavior still need further clarification.

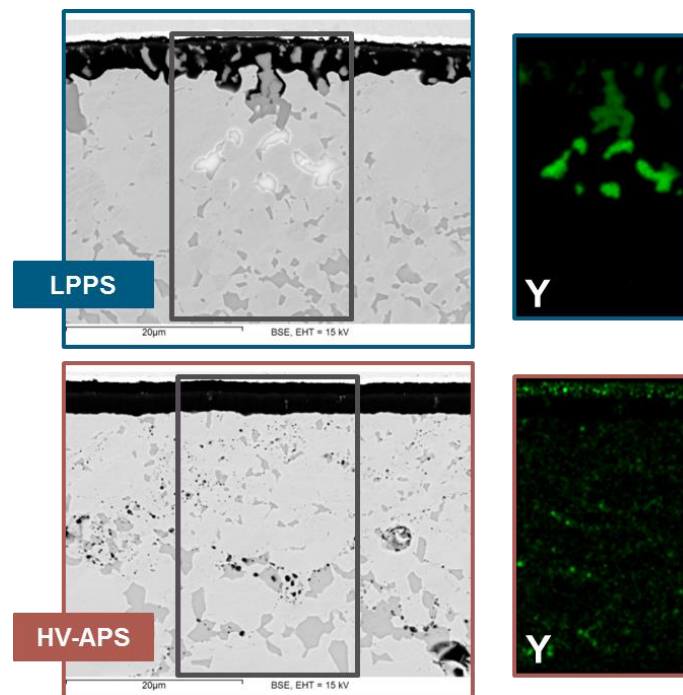


Figure 4. EDX mapping of yttrium distribution near surface zone after 72 h isothermal oxidation (1100 °C) [9].

3. Suspension plasma spraying

Suspension Plasma Spraying (SPS) is a new method to process submicron-sized feedstock powders which are not sufficiently flowable to feed them in dry state [11]. Novel microstructures such as dense vertically cracked or columnar structured ceramic thermal barrier coatings (TBCs) can be obtained [12]. SPS is presently promoted by the development of novel torch concepts with axial feedstock injection such as the Axial III™ plasma torch with three cathodes, anodes, and converging plasma jets, each (Northwest Mettech Corp., Vancouver, Canada).

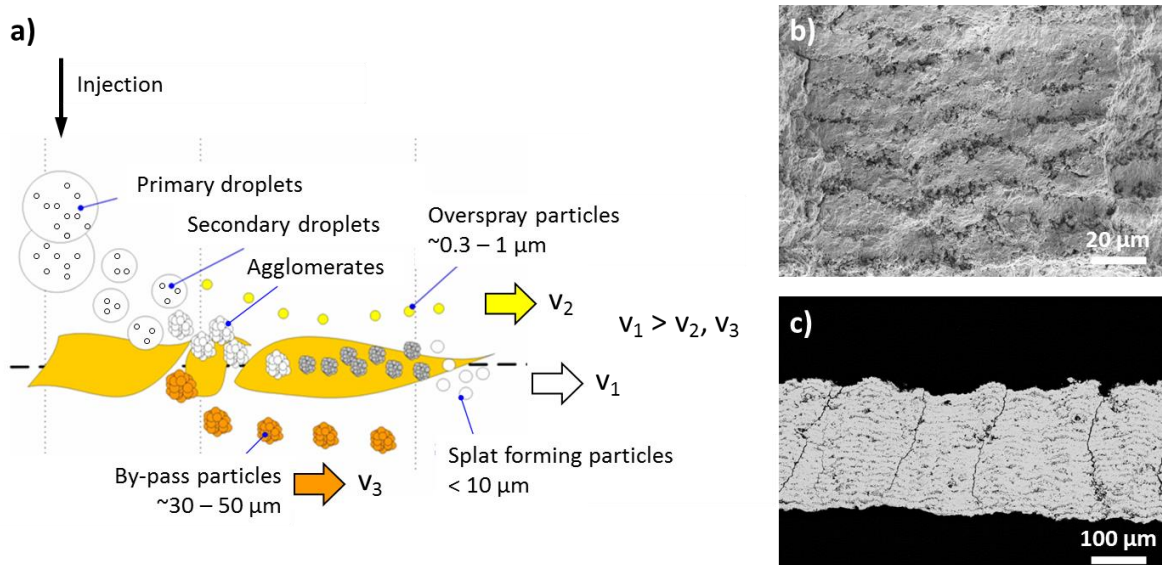


Figure 5. Formation of form highly porous, weakly bonded overspray layers due to radial injection of the suspension feedstock; schematic diagram [13] a), examples: fracture surface b) and polished cross-section c).

Figure 5 illustrates the problem which is associated to SPS with radial injection. After evaporation of the carrier fluid, the solid particles agglomerate. Their trajectories are widely fanned out in radial direction depending on their size. Due to their small inertia, the fine overspray particles do not penetrate deep enough into the hot plasma core so that they are not properly molten. However, they are partly deposited on the substrate on top of each pass and form highly porous, weakly bonded layers. Figure 5 gives two examples. For TBCs, such overspray layers were found to be disadvantageous as they can channel crack propagation and affect the cohesion of the coating. This can be avoided by axial injection of the suspension so that the advantages of nano-sized microstructures can also benefit for TBCs.

Figure 6 shows a columnar structured Y_2O_3 -stabilized ZrO_2 (YSZ)/ $Gd_2Zr_2O_7$ double layer TBC by SPS with axial injection. Coatings were sprayed at 105 kW torch input power on Inconel 738 LC substrates with a MCrAlY bondcoat. The YSZ solid load of the suspension for the TBC was 10 wt% and the feed rate 30 g/min. The solid load of the $Gd_2Zr_2O_7$ -suspension had to be reduced to 5 wt% to achieve columns. This might be related to the larger particle size in the suspension. The detail in Figure 6 shows that the interface between YSZ and $Gd_2Zr_2O_7$ appears free of any interference. The investigation of service life performance and failure modes is still pending.

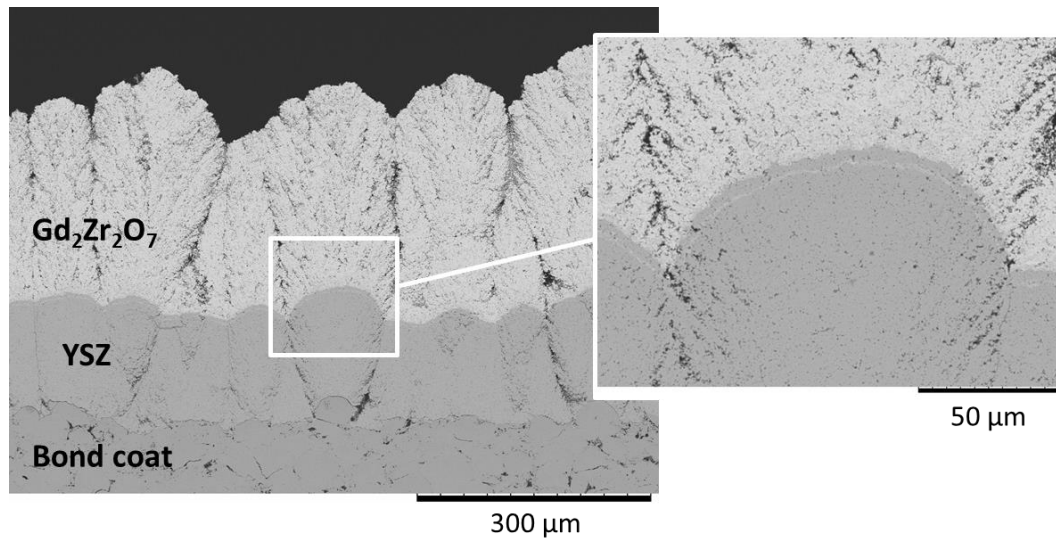


Figure 6. YSZ/Gd₂Zr₂O₇ double layer TBC by SPS with axial injection.

4. Very low pressure plasma spraying

The combination of plasma spraying at very low pressures with enhanced electrical input power led to the development of a process family which is termed Very Low Plasma Spraying (VLPPS) [14]. Applying electrical currents up to 3 kA, an input power level of 150 kW can be achieved. As long as the deposition is dominated by the liquid phase, particular thin and dense coatings can be manufactured. This specific process is termed Low Pressure Plasma Spraying-Thin Film (LPPS-TF). Beyond that, it is even possible to evaporate the feedstock material, if appropriate parameters and powders are applied. In this particular case, the process is termed Plasma Spray-Physical Vapor Deposition (PS-PVD) enabling the manufacture of columnar, strain tolerant microstructures for TBCs. The experiments described in the following were carried out on a Sulzer Metco VLPPS Multicoat system with an O3CP torch (Oerlikon Metco, Wohlen, Switzerland). It resulted from a comprehensive reconstruction of an existing conventional LPPS system. In particular, it was equipped with an additional vacuum pumping unit, a large vacuum blower to provide sufficient pumping capacity at low pressures, enlarged cooling capacity, and new control units.

4.1 Thermal Barrier Coatings by PS-PVD

Two different YSZ microstructures of TBCs manufactured by PS-PVD are given in Figure 7. The corresponding plasma parameters are indicated in the caption. The coating in Figure 7 a) was designed to achieve an increased erosion resistance. However, the thermal conductivity was higher due to the relatively small porosity. In contrast, the coating shown in Figure 7 b) was manufactured at hotter conditions. The highly porous, columnar structure is strain tolerant and exhibits a lower thermal conductivity [15]. However, this is inherently at the expense of erosion resistance.

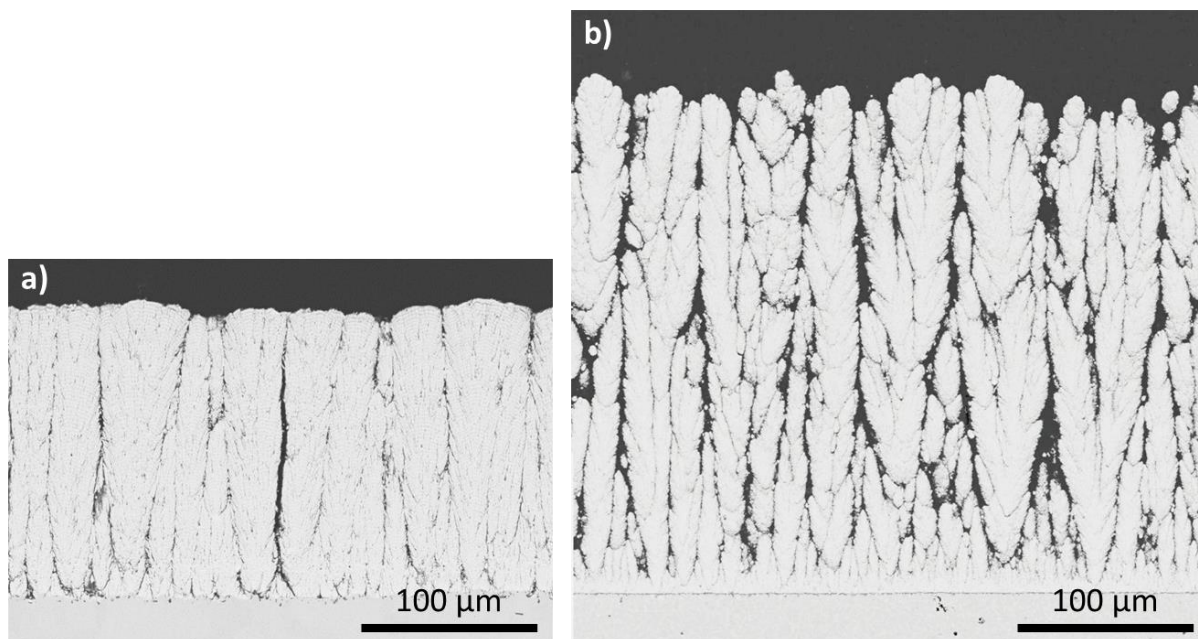


Figure 7. YSZ microstructures for TBCs by PS-PVD; a) plasma parameter 60 slpm He, 35 slpm Ar, 10 slpm H₂, current 2200 A; b) plasma parameter 60 slpm He, 35 slpm Ar, current 2200 Ar [15].

The failure analysis of a TBC system with a YSZ topcoat such as shown in Figure 7 b) is given in Figure 8 after a cyclic thermal gradient test. Details of the experimental setup and procedure can be found elsewhere [16]. The test conditions are indicated in the caption.

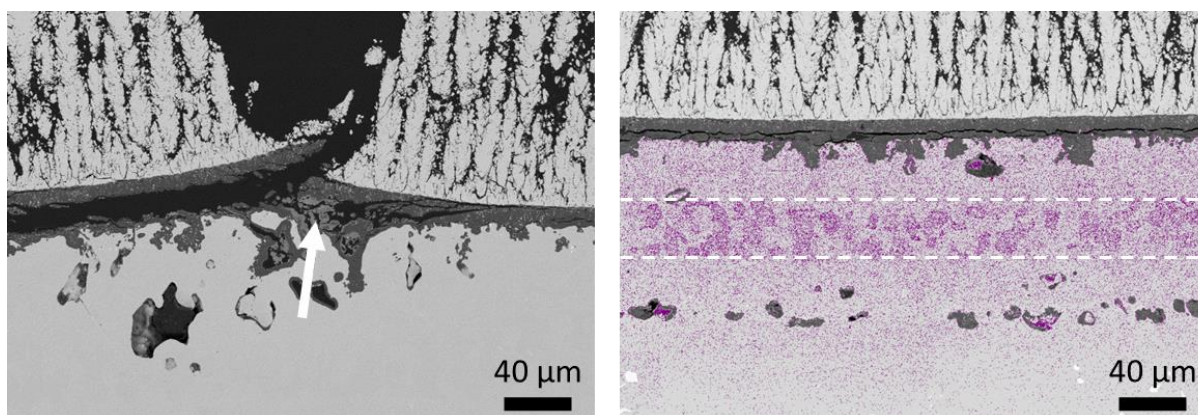


Figure 8. TBC failure analysis after 1185 cycles (~99 h) at cycling conditions $T_{\text{surface}} = 1382^{\circ}\text{C}$, $T_{\text{bondcoat}} \sim 1113^{\circ}\text{C}$; the arrow indicates fast growing transient oxides, the β -phase is coloured to enhance contrast, the dotted lines demarcate the zones of β -phase depletion.

A thick TGO layer was formed which is deep-rooted in the bondcoat by many “pegs”. The ceramic topcoat was locally bulged and behaved highly deformable. No failure within the ceramic TBC was observed indicating a high strain tolerance. For conventional TBCs, such failure mode during cycling is unusual. Below the bulged areas, a non-uniform growth of TGO due to the formation of fast growing transient oxides (Cr_2O_3 , spinel $(\text{Co,Ni})\text{Cr}_2\text{O}_4$) occurred [17]. The bondcoat showed pronounced zones of β -phase depletion. Obviously, the durability of ceramic top coat exceeded the service capability of the bondcoat.

4.2 Oxygen transport membranes by LPPS-TF

The perovskite material $\text{La}_{0.58}\text{Sr}_{0.4}\text{Co}_{0.2}\text{Fe}_{0.8}\text{O}_3$ (LSCF) is a mixed ion and electron conductor applied for oxygen transport membranes and cathodes of solid oxide fuel cells (SOFCs). Due to the large difference between the vapor pressures of its constituents, LSCF is prone to decomposition and inhomogeneous evaporation. Thus, single phase coatings could be obtained by APS only at moderate torch power and short dwell time of the feedstock particles in the plasma jet [18]. However, such coatings are not gastight as required for gas separation membranes.

An alternative approach is LPPS-TF. The feedstock was an agglomerated powder with $d_{50} = 10 \mu\text{m}$ consisting of single phase rhombohedral perovskite; the feed rate was 20 g min^{-1} . The membranes were sprayed directly on a porous, sintered NiCoCrAlY substrate at a plasma torch input power of 90 kW and an Ar/He plasma gas mixture. The chamber pressure was 200 Pa and a small amount of extra O_2 was introduced into the chamber to maintain the LSCF stoichiometry. The example given in Figure 9 demonstrates that the large substrate porosity of approx. 40% could be closed effectively. The detail reveals that the splats were flattened widely so that voids and pores were levelled out [19].

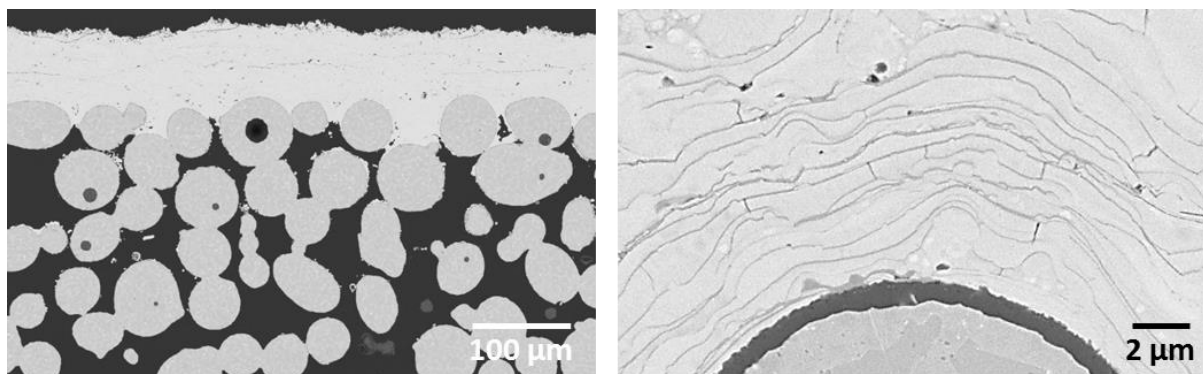


Figure 9. Thin and gastight LSCF membrane on a porous MCrAlY substrate by LPPS-TF [19].

Such LSCF coatings meet the requirements on oxygen separation membranes. They are dense (porosity 0.4%), gastight, and thin (approx. $50 \mu\text{m}$). The metal substrate is a mechanical stable alternative to conventional ceramic supported cells. No subsequent sintering procedure is needed; hence, no shrinking occurs as on wet chemical routes [20]. An oxygen permeation test for 300 h at temperatures up to 1000°C revealed an oxygen permeation rate of 5.3 ml/min cm^2 which is amongst the highest fluxes measured up to now for LSCF [21]. The scalability of crack-free samples was preliminary demonstrated up to a diameter of 105 mm.

4.3 Electrolytes for solid oxide fuel cells

Metal supported SOFCs were manufactured by a combination of APS and LPPS-TF [22]. The substrate was a Fe-Cr alloy with a porosity of 40%. The anode was deposited by APS containing YSZ unmelted globules in a Ni/NiO grain matrix at a porosity of 9%. The YSZ electrolyte was manufactured by LPPS-TF with a thickness of $26 \mu\text{m}$ and 2% porosity. For the cell tests, a simple LSCF cathode was screen-printed which was kept non-sintered.

Figure 10 shows the metal supported fuel cell assembly and a cross-section at the working electrode site after testing. Air-tightness (anode & electrolyte) as well as a good contact at the metal support/anode and anode/electrolyte interfaces were achieved. The contact at the cathode/electrolyte interface however still needs improvement.

The cell test at 817°C resulted in a good open-circuit voltage (OCV) of 1.033 V. At the same temperature, the current density was 1.380 A cm^{-2} at 0.7 V corresponding to a power density of 0.976 W cm^{-2} . These values are higher than known from literature for solid oxide fuel cells with thermally sprayed functional layers. Details can be found elsewhere [22]. The excellent cell

performance was attributed to the high ionic conductivity and good inter-splat contact in the electrolyte layer, even though it is not absolutely dense. Further optimization potential is suggested with respect to powder processing in order to reduce the still existing porosity and the thickness of the membrane.

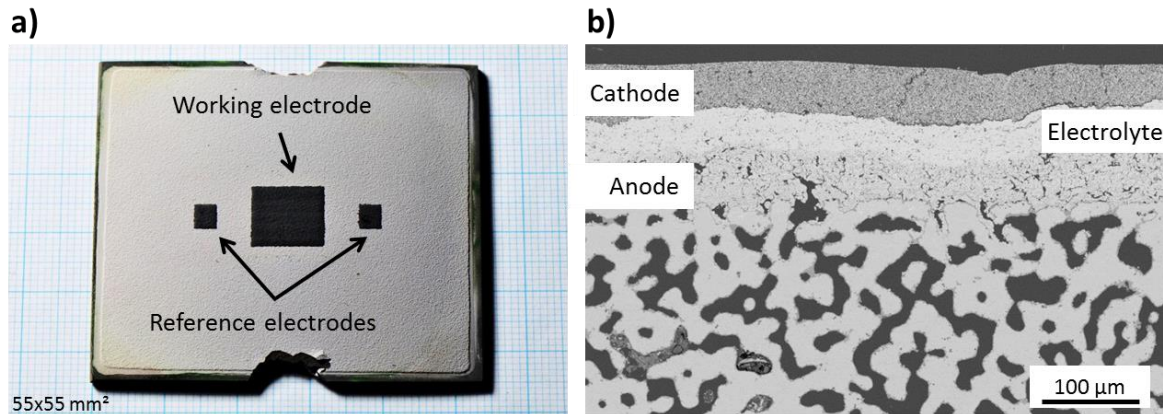


Figure 10. a) Metal supported solid oxide fuel cell by APS/LPPS-TF; b) cross section of anode, electrolyte, and cathode assembly at the working electrode site after testing.

5. Summary and conclusions

In this work, recent developments of plasma spraying techniques are described with respect to specific demands in energy technology. Three processes and some typical applications are given as examples. HV-APS parameters were developed for the TriplexPro™-210 torch with a 5 mm high velocity nozzle. The best MCrAlY microstructures were obtained using a fine powder with $d_{50} = 14 \mu\text{m}$. Although the spray conditions were generally cold, reasonable deposition efficiencies and rather dense coatings were achieved. The oxidation rates of free standing HV-APS coatings were lower than those of LPPS reference coatings. Far less Y incorporation in the oxide scale and a better oxide scale adherence were observed. The reason for the superior oxidation performance was suggested to be related to the unique distribution of Y-rich nano-sized oxide precipitates in the coatings.

TBCs with different structures, such as vertical cracked and columnar, can be manufactured by SPS axial suspension injection. A columnar structured YSZ/ $\text{Gd}_2\text{Zr}_2\text{O}_7$ double layer system was given as an example. The investigation of service life performance and failure modes is still pending.

LPPS-TF and PS-PVD are significantly different from spraying under atmospheric conditions. Novel structural features can be achieved. One example are highly strain tolerant columnar structured TBCs by PS-PVD with excellent adhesion to the bondcoat. Other examples are dense and effective oxygen transport membranes by LPPS-TF. Thin and gastight LSCF thin films exhibiting high oxygen permeation rates were deposited directly on porous metallic supports. Finally, an air-tight metal supported SOFC assembly was obtained by a combination of APS and LPPS-TF. This cell showed a good OCV and an excellent power density.

Acknowledgments

The cooperation on HV-APS with A. Barth, M. Gindrat, and H.-M. Höhle (Oerlikon Metco, Wohlen) is gratefully acknowledged. The research on the oxygen transport membranes has partly received funding from the European Community's Seventh Framework Programme (FP7/2007-2013) under grant agreement no. 241309 (Project acronym: DEMOYS). The oxygen permeation measurements of the LSCF membranes were carried out by J. Serra and J. Garcia (CSIC, Valencia). The SOFC cell tests were performed by A. Weber (KIT, Karlsruhe).

References

- [1] Mauer G, Jarligo M O, Mack D E and Vaßen R 2013 Plasma-Sprayed Thermal Barrier Coatings: New Materials, Processing Issues, and Solutions *J. Therm. Spray Technol.* **22** 646-58
- [2] Toscano J, Vaßen R, Gil A, Subanovic M, Naumenko D, Singheiser L and Quadackers W J 2006 Parameters affecting TGO growth and adherence on MCrAlY-bond coats for TBC's *Surf. Coat. Technol.* **201** 3906-10
- [3] Naumenko D, Shemet V, Singheiser L and Quadackers W J 2009 Failure mechanisms of thermal barrier coatings on MCrAlY-type bondcoats associated with the formation of the thermally grown oxide *J. Mater. Sci.* **44** 1687-703
- [4] Mauer G, Sebold D and Vaßen R 2014 MCrAlY Bondcoats by High-Velocity Atmospheric Plasma Spraying *J. Therm. Spray Technol.* **23** 140-6
- [5] Mauer G, Vaßen R and Stöver D 2007 Controlling the oxygen contents in vacuum plasma sprayed metal alloy coatings *Surf. Coat. Technol.* **201** 4796-9
- [6] Patterson T, Leon A, Jayaraj B, Liu J and Sohn Y H 2008 Thermal cyclic lifetime and oxidation behavior of air plasma sprayed CoNiCrAlY bond coats for thermal barrier coatings *Surf. Coat. Technol.* **203** 437-41
- [7] Shibata M, Kuroda S, Murakami H, Ode M, Watanabe M and Sakamoto Y 2006 Comparison of Microstructure and Oxidation Behavior of CoNiCrAlY Bond Coatings Prepared by Different Thermal Spray Processes *Mater. Trans.* **47** 1638-42
- [8] Rajasekaran B, Mauer G and Vaßen R 2011 Enhanced Characteristics of HVOF-sprayed MCrAlY Bond Coats for TBC Applications *J. Therm. Spray Technol.* **20** 1209-16
- [9] Mauer G, Sebold D, Vaßen R, Hejrani E, Naumenko D and Quadackers W J 2016 Impact of processing conditions and feedstock characteristics on thermally sprayed MCrAlY bondcoat properties *Surf. Coat. Technol.*
- [10] Evans H E 1995 Stress effects in high temperature oxidation of metals *Int. Mater. Rev.* **40** 1-40
- [11] Killinger A, Gadow R, Mauer G, Guignard A, Vaßen R and Stöver D 2011 Review of New Developments in Suspension and Solution Precursor Thermal Spray Processes *J. Therm. Spray Technol.* **20** 677-95
- [12] Guignard A, Mauer G, Vaßen R and Stöver D 2012 Deposition and Characteristics of Submicrometer-Structured Thermal Barrier Coatings by Suspension Plasma Spraying *J. Therm. Spray Technol.* **21** 416-24
- [13] Siegert R 2006 A Novel Process for the Liquid Feedstock Plasma Spray of Ceramic Coatings with Nanostructural Features. PhD thesis Ruhr University Bochum. In: *Berichte des Forschungszentrums Jülich vol. 4205*, (Jülich: Forschungszentrum Jülich)
- [14] Mauer G, Gindrat M and Smith M F 2016 Very Low Pressure Plasma Spraying (VLPPS), including PS-TF, PS-PVD, and PS-CVD. In: A. Vardelle et al., The 2016 Thermal Spray Roadmap *J. Therm. Spray Technol.* **25** 1383-8
- [15] Mauer G 2014 Plasma Characteristics and Plasma-Feedstock Interaction Under PS-PVD Process Conditions *Plasma Chem. Plasma Process.* **34** 1171-86
- [16] Traeger F, Rauwald K-H, Vaßen R and Stöver D 2003 Thermal Cycling Setup for Testing Thermal Barrier Coatings *Adv. Eng. Mater.* **5** 429-32

- [17] Rezanka S, Mauer G and Vaßen R 2014 Improved Thermal Cycling Durability of Thermal Barrier Coatings Manufactured by PS-PVD *J. Therm. Spray Technol.* **23** 182-9
- [18] Harris J and Kesler O 2009 Atmospheric Plasma Spraying Low-Temperature Cathode Materials for Solid Oxide Fuel Cells *J. Therm. Spray Technol.* **19** 328-35
- [19] Jarligo M O, Mauer G, Bram M, Baumann S and Vaßen R 2014 Plasma Spray Physical Vapor Deposition of $\text{La}_{1-x}\text{Sr}_x\text{Co}_y\text{Fe}_{1-y}\text{O}_{3-\delta}$ Thin-Film Oxygen Transport Membrane on Porous Metallic Supports *J. Therm. Spray Technol.* **23** 213-9
- [20] Mauer G, Jarligo M O, Rezanka S, Hospach A and Vaßen R 2015 Novel opportunities for thermal spray by PS-PVD *Surf. Coat. Technol.* **268** 52-7
- [21] Marcano D, Mauer G, Sohn Y J, Vaßen R, Garcia-Fayos J and Serra J M 2016 Controlling the stress state of $\text{La}_{1-x}\text{Sr}_x\text{Co}_y\text{Fe}_{1-y}\text{O}_{3-\delta}$ oxygen transport membranes on porous metallic supports deposited by plasma spray–physical vapor process *J. Membr. Sci.* **503** 1-7
- [22] Marcano D, Mauer G, Vaßen R and Weber A 2016 Manufacturing of high performance solid oxide fuel cells (SOFCs) with atmospheric plasma spraying (APS) and plasma spray-physical vapor deposition (PS-PVD) *Surf. Coat. Technol.*